JMEPEG (2010) 19:643–649
DOI: 10.1007/s11665-009-9528-1

1059-9495/$19.00

Preparation and Characterization of Carbon Microfiber Through Shear Pulverization Using Pan-Mill Equipment

Feng Shi, Canhui Lu, and Mei Liang

(Submitted October 19, 2008; in revised form July 14, 2009)

Carbon microfiber was prepared through shear pulverization using the self-designed pan-mill type equipment at ambient temperature from short carbon fiber (CF). The effects of shear stress on structure transformations, particles size, microfiber morphology, surface functional groups and crystalline properties during pulverization were studied by laser diffraction particle size analyzer, scanning electron microscopy (SEM), Fourier transform infrared spectroscopy (FT-IR), x-ray photoelectron spectroscopy (XPS) and wide-angle x-ray diffraction (WAXD), respectively. SEM analysis indicated that CF was milled into microfiber due to the strong shear and squeezing force. The average particle size of carbon microfiber was reduced to 12.7 μm and specific surface area was increased to 0.6 m^2/g after 40 milling cycles. FT-IR and XPS analyses showed that the oxygen-containing groups increased after shear pulverization, and WAXD results illustrated that shear stress offered by mill discs had an obvious damage on the crystal structure of CF, leading to a decrease of crystallinity. Thermal analysis showed that carbon microfiber exhibited good thermal stability. The pan-milling shear pulverization technique is an environment-friendly and efficient method for preparing carbon microfiber.

Keywords carbon fiber, mechanochemistry, microfiber, morphology, pan-milling

1. Introduction

Carbon microfiber is applied to the development of hydrogen storage (Ref 1, 2) and efficient field emission cathodes (Ref 3) for applications such as x-ray tubes (Ref 4), light sources (Ref 5) and flat panel displays (Ref 6). Because of their high mechanical strength, high electrical and thermal conductivity, such carbon microfiber has also been considered as ideal reinforcing fillers in polymer composites with high performance and multi-function (Ref 7-10). The particular advantage of microfiber is that it can be incorporated more easily into the polymer, providing more filling volume and interfacial surface area (Ref 11). Furthermore, due to its suitable size, carbon microfiber polymer composites can be processed using conventional processing techniques, such as extrusion and injection molding (Ref 12).

Carbon microfiber can be prepared from carbon fiber by some mechanical milling techniques, such as mechanical knife mill, ball mill, etc. Among these, mechanochemical processing based on high-energy ball milling is considered as a versatile, low-cost technique for the manufacture of carbon microfiber (Ref 13, 14). However, enlargement of production scale and continual operation are two challenging exploitations for commercial application of high-energy ball-milling technique. The pulverizing efficiency of high-energy ball mill is determined by the collision probability of fiber and milling media (balls), the impact force, the oscillating frequency and amplitude of the equipment. High ball/fiber ratio and long milling time are required (Ref 15). For example, Sheshin (Ref 3) milled carbon fiber to prepare field emission cathodes materials with a milling time from 3 to 16 h. Welham et al. (Ref 16) reported that their sample mass was about 7 g for each milling, and took a long time (100 h) to make product.

For the purpose of enhancing the efficiency of ready-made pulverizing equipment, a novel pulverizing equipment, pan-mill type equipment was designed and set up in our laboratory (Ref 17, 18). A digital camera picture of the equipment is shown in Fig. 1. Figure 2 is a schematic diagram of the inlaid mill-pan, which is also the innovation key part of the equipment. The main structural parameters of the pan-mill are radius, R, division number, n, slot number in each division, m, bevel angle, α, and slot top width, δ. Theoretical analysis demonstrates that this equipment has excellent pulverizing and mixing effect on various materials due to the ingenious design. Functioning like a pair of three-dimensional scissors, pan-mill type equipment can exert on materials fairly strong squeezing force in normal direction and shear stress in both radial and tangential directions. Both particle size reduction and mechanochemical reaction will occur during milling process. Our self-designed equipment displays high efficiency in pulverizing, dispersing, mixing as well as activating for material processing (Ref 15). We have successfully prepared kinds of polymer powders by this equipment, including ultrafine polypropylene/iron composite powder (Ref 19), PEEK powder (Ref 20), hardwood cellulose powder (Ref 21), etc.

In this study, we introduced the pan-milling technique to prepare carbon microfiber. The changes of structure and morphology during milling were studied. The pan-milled

Feng Shi, Canhui Lu, and **Mei Liang**, State Key Laboratory of Polymer Materials Engineering, Polymer Research Institute, Sichuan University, Chengdu 610065, China. Contact e-mail: canhuilu@scu.edu.cn.

Fig. 1 Digital camera picture of pan-mill equipment

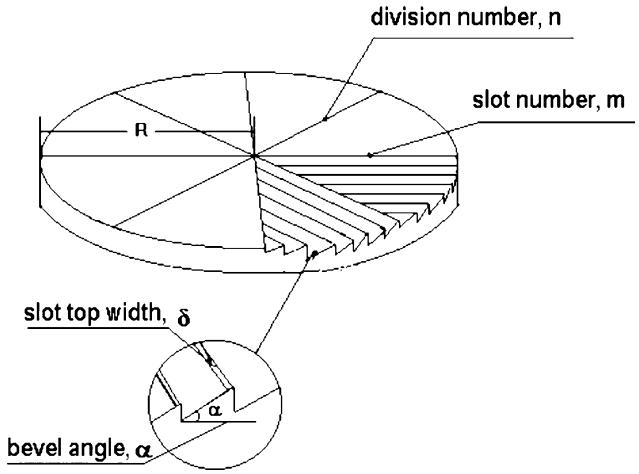

Fig. 2 Schematic diagram of inlaid mill-pan

carbon microfiber with high specific surface area ratio, more oxygen-containing groups are suitable for subsequent applications such as polymer fillers for injection and extrusion, reinforced coatings, field emission cathodes and hydrogen storage materials. Compared with conventional ball milling, pan-milling approach was proved to be efficient, and easy to be industrialized for preparing carbon microfiber.

2. Experimental

2.1 Materials

Carbon fiber was purchased from Nantong Senyou Carbon Fiber Co., Ltd. (Jiangsu, China). This carbon fiber derived from polyacrylonitrile (PAN) precursor was approximately 8 μm in diameter and 6 mm in length.

2.2 Pan-Mill Type Equipment

Figure 1 is a simple scheme of the pan-mill type equipment and Fig. 2 shows the structure of its key part, the milling pans. A chain transmission system and a screw pressure system are set to regulate the rotation speed of moving pan and imposed load, respectively, which can strictly control two major dynamic parameters, velocity and force, during milling. Cooling water flows through the hollow interior of the moving pan to take away the heat generated during milling. Milling temperature is adjustable by controlling the flux of the cooling water. Milling process can be described as follows. The materials are fed to the center of the pan from the inlet, and move along a spiral route toward edge of the pan till they come out from the outlet, thus one cycle of milling is finished (Ref 17).

2.3 Preparation of Carbon Microfiber

Short carbon fiber was fed in inlet which set in the front of the static pan. Milled fiber was discharged from the brim of the pans, and then collected from the outlet for the next pan-milling cycle. The whole milling process was controlled by certain rotating speed and pan gap at ambient temperature.

2.4 Measurement and Characterization

2.4.1 Size and Specific Surface Area Analysis. The particle size (mean diameter) and particle size distribution of carbon microfiber were measured by Masterizer 2000 Laser Particle Analyzer. The measurement range of size analysis is 0.02-2000 μm. An appropriate amount of each sample was dispersed in ethanol (ρ = 0.789-0.791 g/mL, AR), stirred at a pumping speed of 2400 rpm. The data were obtained by breaking up the flocculates ultrasonically. Then, the particle size and particle size distribution were calculated from the light scattering pattern, and the specific surface area of carbon microfiber could be estimated simultaneously.

2.4.2 Morphology Observation. The morphology of carbon microfiber in different milling cycles was observed under a scanning electron microscope (JEOL JSM-5600, Japan). A thin layer of Pd-Au alloy was coated on the specimens prior to measurement to prevent charging on the surfaces. SEM was operated at an accelerating voltage of 20 kV. The representative value of the average fiber length was measured directly from SEM photos using the ImageJ software, version 1.40 (Ref 22).

2.4.3 FT-IR Analysis. FTIR spectra were studied by a Nicolet Nexus 670 spectrometer with a resolution of 4 cm^{-1}, ranging from 4000 to 400 cm^{-1}. The samples for analysis were prepared as follows: 1 mg of short carbon fiber and carbon microfiber was mixed with 200-300 mg KBr, respectively. The required discs were then obtained in a standard mold under a pressure of 4 MPa. Both testing samples and KBr were dried before disc preparation and were subjected to FTIR analysis immediately afterwards.

2.4.4 XPS Analysis. The x-ray photoelectron spectroscopy (XPS) analysis was carried out in a XSAM800 (Kratos, UK), using a monochromatic Al Kα x-ray source, at a base pressure of 6.7×10^{-7} Torr or lower. All specimens were analyzed at a photoelectron take-off angle of 45° and high resolution spectra were obtained. The XPS raw data were compiled and analyzed using the XPSPeak Software, version 4.1 (Ref 23). For calibration purposes, the C_{1s} electron binding

energy corresponding to graphitic carbon was referenced at 284.6 eV (Ref 23). Atomic ratios were calculated from the data after Shirley background subtraction.

2.4.5 WAXD Analysis. Wide-angle x-ray diffraction (WAXD) measurements were performed in a Philips Analytical X'Pert X-diffractometer, using Co Kα radiation at λ = 0.1788 nm (40 kV, 40 mA). The samples were compacted to small mats for measurements. WAXD data were collected from 2θ = 15-80° with a step interval of 0.02°. The crystal form can be expressed.

2.4.6 Thermal Analysis. Thermogravimetric analysis (TGA) was conducted on TGA Q500 analyzer (TA Instruments). Samples of about 5 mg were placed in an open alumina crucible. Temperature programs for dynamic test were from 40 to 1000 °C at a heating rate of 20 °C/min. The measurements were operated under a nitrogen purge (100 mL/min).

3. Results and Discussion

3.1 Size Reduction During Pan-Milling and Specific Surface Area Analysis

Under the shear force field, carbon fiber deforms firstly. If the applied stresses are strong enough, flaws may appear due to stress concentrations at the weak point on fiber surface (cracks, defects and amorphous regions). Then, flaws can spread gradually into inner fiber. When the applied energy exceeds the critical energy which plastic deformation demands, fiber fractures with drastic decrease of fiber length. Figure 3 shows the average particle size and their specific surface area of short carbon fiber versus pan-milling cycles, respectively. The result indicates that the average particles size decreases almost linearly with increasing milling cycle. As the pan-milling cycle increases, the decrease of fiber length slows down due to the diminishment of the surface weakness. Besides, the increase of specific surface area, van der Waals force and electrostatic force impart to the milled microfiber a strong tendency to agglomerate. At the final stage of mechanochemical milling, pulverization and agglomeration come to an equilibrium state. The average particles size is reduced to 12.7 μm and hardly changed after 40 milling cycles. The specific surface area

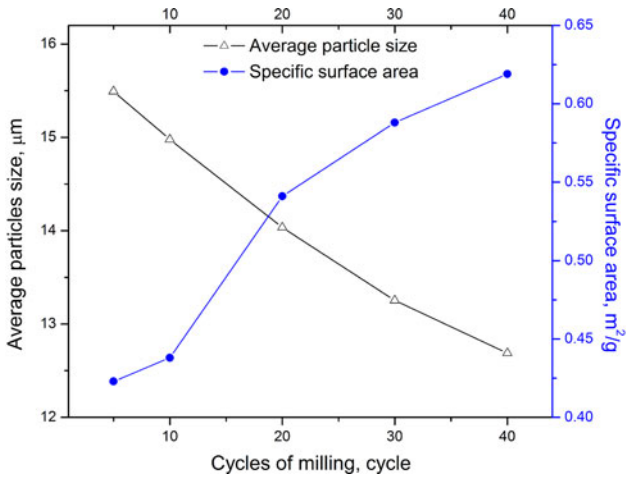

Fig. 3 Effect of pan-milling on particle size and specific surface area of short CF

increases to 0.6 m^2/g after 40 milling cycles, indicating fibers disperse and break down, some crevices appear on the surface of fiber after milling. The crevices and the cut edges can provide more new surface area, which is consistent with the SEM graph as shown in Fig. 4(d).

3.2 Morphological Observation

The surface texture and morphology of carbon fiber after pulverization in pan-milling were studied. Figure 4(a) shows the original short carbon fiber without any treatment. After milling, as shown in Fig. 4(b), short carbon fiber was cut, deformed and squeezed into microfiber. As the milling cycle increases, the particle size and fiber length decrease clearly. Although carbon microfiber appears to be powder in macroscopy, it actually preserves the properties and structures of carbon fiber with certain length-diameter ratio (Ref 4). Figure 4(c) and (d) shows the detailed surface morphology of original short carbon fiber and milled carbon fiber, respectively. A close SEM examination of original carbon fiber reveals that its surface is fairly smooth except for the presence of slight shallow gutters oriented along the fiber axes. Smooth surface is chemically inert, and manifests weak interfacial interactions, resulting in poor adhesion between fibers and matrix (Ref 24). After 40 milling cycles, the high magnification view (×3000) of fiber surface shows that the longitudinal gutters deepen and the surface roughness increases (Fig. 4d). And some deep micro pits appear in crevices of fiber, which may suggest that there are more defects in the crevices where the formation of micro pits occurs preferably (Ref 25). The increase of specific surface areas and the occurrence of micro pits can enhance the interfacial contact area and adhesion between fibers and polymer matrix for composites.

Figure 5 illustrates the length distribution of carbon microfiber after 5 milling cycles (Fig. 5a) and 40 milling cycles (Fig. 5b). The original short carbon fiber, made by means of a series of razor blades strung on a threaded rod, is approximately 6 mm in length. It can be seen that only after 5 milling cycles, the length sharply decreases to no more than 170 μm and the average length is 31.0 μm. After 40 milling cycles, the length distribution shifts to the small zone regularly. The length distribution becomes narrower and the fiber length ranges between 4 and 60 μm with an average length of 17.3 μm, indicating that the strong squeezing, shearing, and pulverizing action generated by pan-mill type equipment can effectively break up carbon fiber in order to produce carbon microfiber.

3.3 FT-IR Analysis

As analyzed before, polymer mechanochemically processed in open air was susceptible to oxygen, which would introduce polar groups onto molecular chains (Ref 26, 27). FT-IR analysis, which is a convenient method to obtain the structure change information, was employed to investigate whether any new functional groups were generated during pan-milling process. Figure 6 shows the FT-IR spectra of carbon fiber before and after milling. The curve marked as (a) is for the original carbon fiber. It is a typical FT-IR spectrum of carbon fiber (Ref 28), and the peak at about 1618 cm^{-1} in the spectrum may be associated with a stretching vibrations of aromatics (C=C) and/or the bending vibrations of physisorbed H_2O (Ref 29). After 40 milling cycles (marked as b), it is evident that the intensity of each peak changed obviously, demonstrating structure transformation induced by mechanical stress

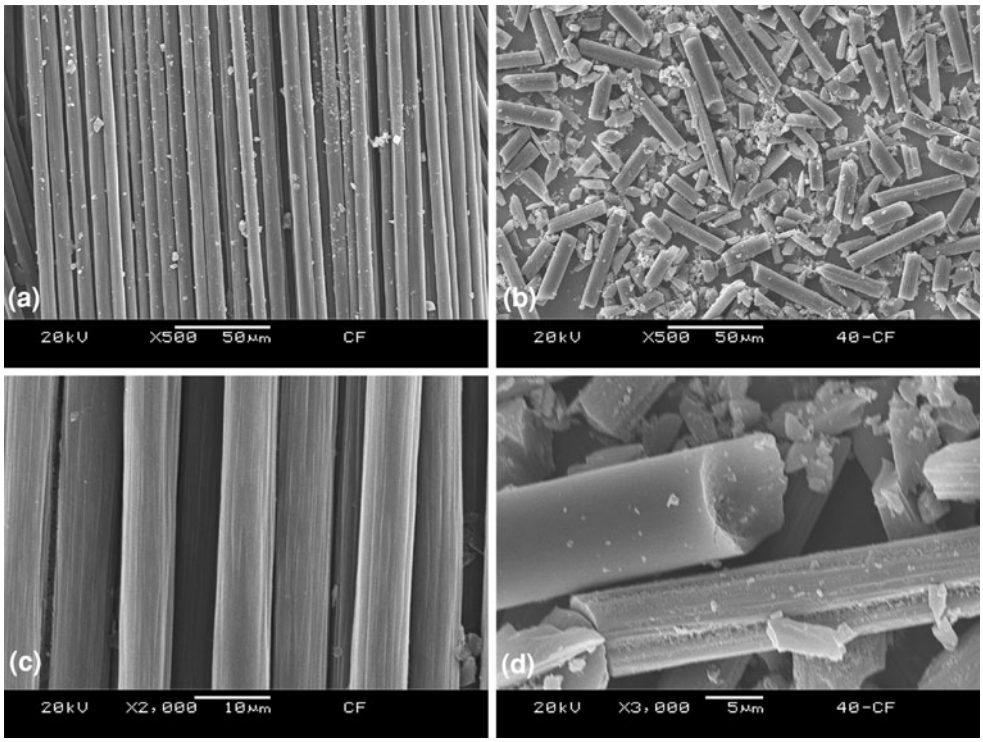

Fig. 4 SEM photos of short CF: (a) original short CF, × 500; (b) short CF milled 40 cycles, × 500; (c) original short CF, × 2000; (d) short CF milled 40 cycles, × 3000

during pan-milling. The transmittance at 1116 cm^{-1} characterizes C-O-C stretching vibration while 3433 cm^{-1} characterizes O-H stretching vibration. After milling, these peaks of oxygen-containing functional groups were enhanced clearly due to the generation of C-O-C functional groups and oxygen-containing carbon ring groups (e.g., phenolic hydroxyl group, quinonoid carbonyl group, etc.) (Ref 30, 31).

3.4 X-Ray Photoelectron Spectroscopy

XPS experiments were performed on both original and milled short carbon fiber to characterize the surface composition. Table 1 shows the surface element analysis results of samples obtained from high-resolution XPS. Based on the survey, the atom percentage of C_{1s} (BE = 285 eV), O_{1s} (BE = 532 eV) and N_{1s} (BE = 399 eV) in fiber surface can be calculated from peaks intensities. Original carbon fiber displays an O_{1s}/C_{1s} ratio of 0.11. The oxygen-containing functional groups of raw materials are attributed to the residual groups on the polymeric precursor (Ref 32). When carbon fiber is milled in open circumstances, oxygen-containing functional groups can be introduced through mechanochemical reactions, resulting in a higher O_{1s}/C_{1s} ratio on the surface which is due to the new-formed oxygen-containing functional groups. Since XPS analyzes only the outer 50 Å of the fiber, the increasing oxygen groups may mainly exist on the void surfaces and slits which are formed during pan-milling.

Figure 7 shows the comparison of high-resolution C_{1s} intensity of original (Fig. 7a) and milled carbon fiber (Fig. 7b). High-resolution XPS C_{1s} spectra of carbon-based oxides can be fitted to six components according to the oxygen atoms bonded to carbon (Ref 33, 34). Graphitic carbon correspond to the graphitic linkage of carbon fiber (284.6 eV); β-carbon and -C-N (285.4 eV); carbon present in phenolic, alcohol, ether or C=N groups (286.1-286.3 eV); carbonyl or quinine groups (287.3-287.6 eV); ester groups (288.1-289.1 eV) and carbon present in carbonate groups and/or adsorbed CO and CO_2 (290.4-290.8 eV). The percentages of graphitic and functional carbon atoms are calculated. It can be seen that the C_{1s} spectra become more asymmetric and broader toward higher binding energy, consisting with the rearrangement in the relative proportion of oxygen-containing functional groups after milling (Fig. 7b). There is a significant decrease in the relative content of graphitic carbon (BE = 284.6 eV), whereas the relative content of carbon bonded to oxygen-containing functional groups increases, which are mainly attributed to the increase of ether (BE = 286.2 eV) and carboxyl or ester (BE = 287.6 eV) type groups.

3.5 X-Ray Diffraction Patterns

Shear stress is the main reason for material breakage during solid-state pulverization at room temperature. The energy acting upon carbon fiber converts into the following forms: macro structure deformation (pulverization and aggregation), heat caused by friction between materials and structural changes in molecule level (such as the breakage of intermolecular and intramolecular hydrogen bonding, fracture of lattice structure and breakage of chain segment). X-ray diffraction patterns obtained before and after milling are shown in Fig. 8. The original short carbon fiber marked as (a) exhibits a sharp high peak at 2θ closed to 30.5°, which is assigned to the [002] lattice plane of hexagonal graphite crystal, and the weaker diffraction at 2θ closed to 52.0° is for the [101] lattice plane (Ref 35). An obvious change of carbon fiber milled for 40 cycles (marked as b) is found in the reflection [002], which

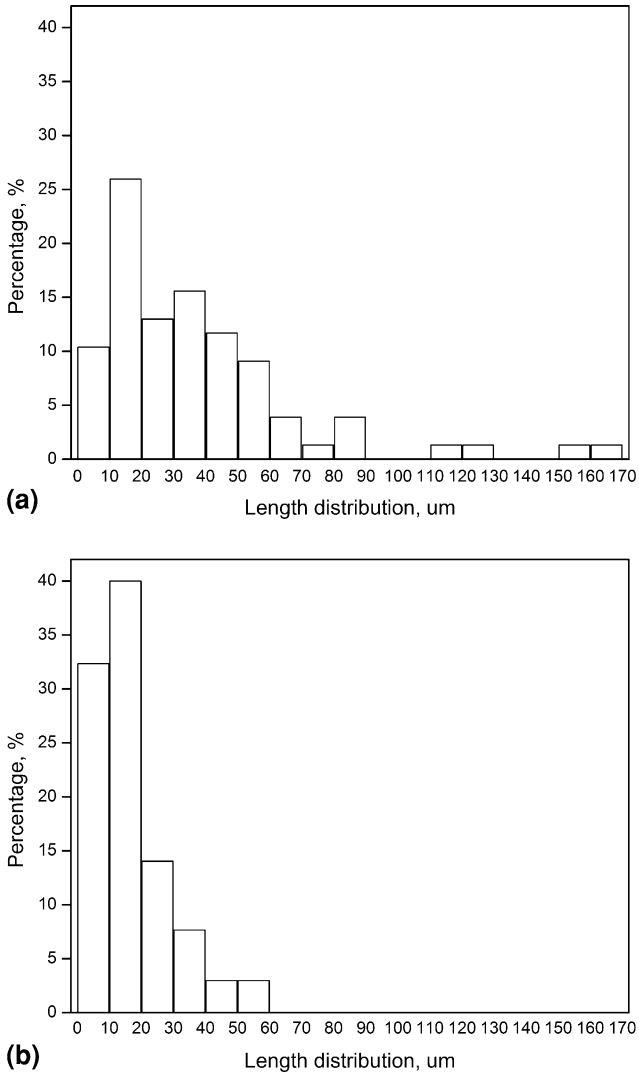

Fig. 5 Length distribution of carbon microfiber: (a) milled 5 cycles; (b) milled 40 cycles

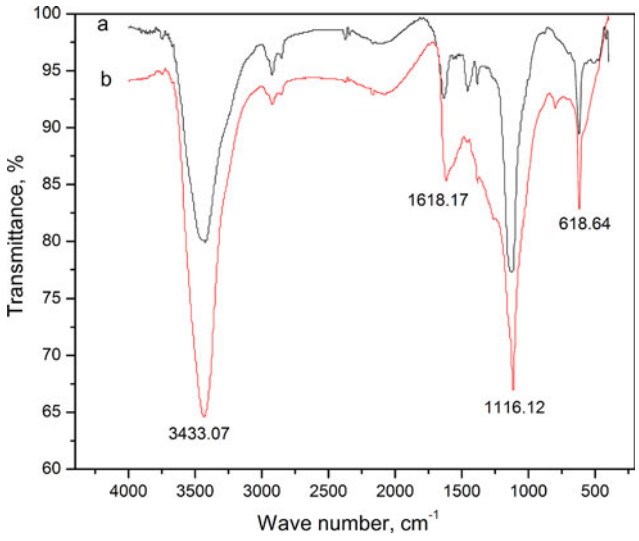

Fig. 6 FT-IR analysis of (a) original short CF and (b) short CF milled 40 cycles

Table 1 XPS surface element analysis of original and milled CF

Carbon fiber	C, %	O, %	N, %	O/C	N/C
Original	87.8	10.1	2.1	0.11	0.02
Milled 40 cycles	83.3	12.5	4.2	0.15	0.05

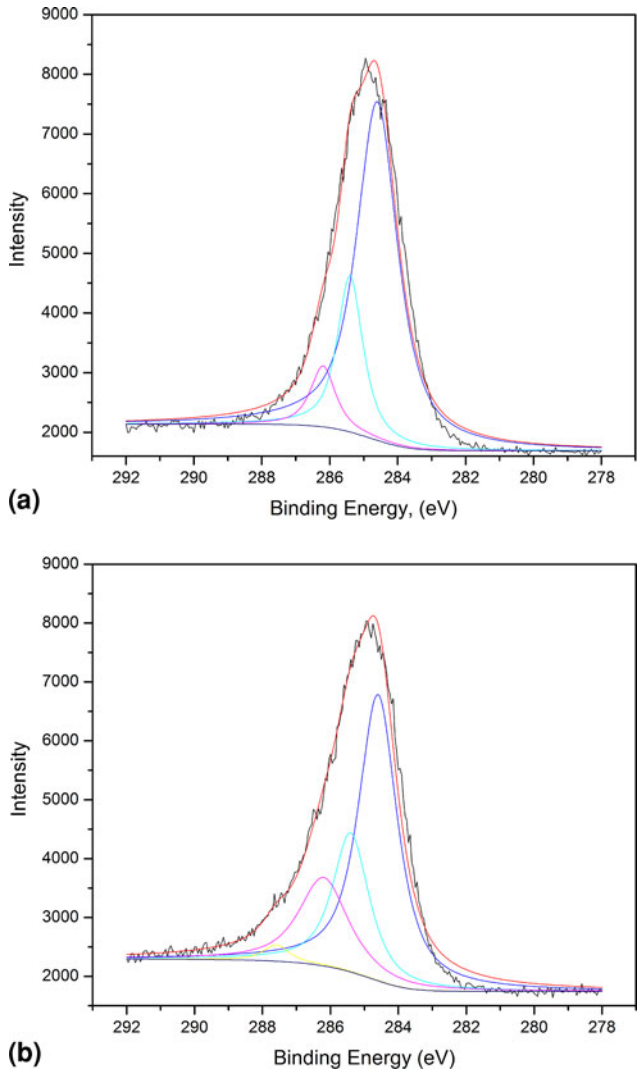

Fig. 7 XPS C_{1s} spectra: (a) original short CF; (b) short CF milled 40 cycles

becomes wider and less intensive. This could be regarded as the reduction of crystalline ordered scattering units because of a breakage of original crystallites and a considerable distortion of the three-dimensional crystalline order. However, crystal type of carbon fiber did not alter after pan-milling.

3.6 Thermal Analysis

The thermal degradation of carbon fiber before and after milling was characterized by TGA. Figure 9 shows a continuous trace of weight change in sample as a function of temperature ranging from 40 to 1000 °C under nitrogen. It is clear that both original and milled carbon fiber begin to lose

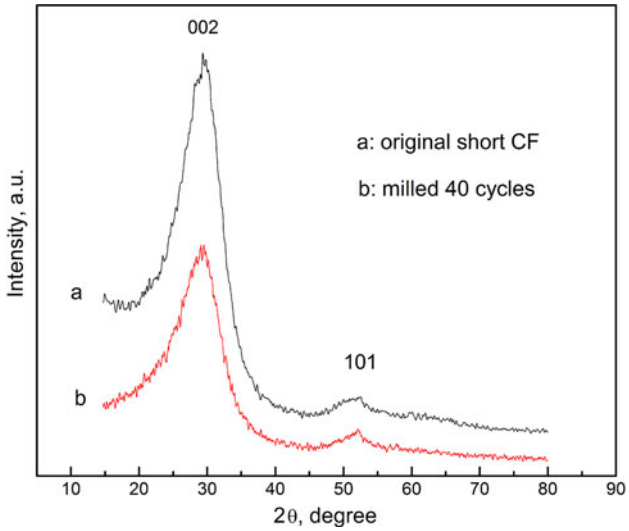

Fig. 8 WAXD analyses of short CF before and after milling

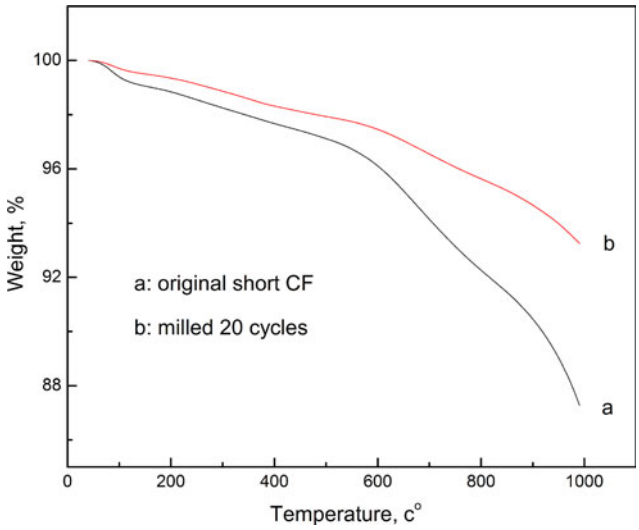

Fig. 9 TGA curves of short CF before and after milling

weight slightly from room temperature, which is probably because of evaporation of moisture at around 100 °C from the hydroxyl groups. At 500 °C, the weight losses of original carbon fiber are due to the removal of organic sizing on fiber surface. With the increase of temperature, the removal of H, O, and N atoms from the residual nitrogen and oxygen in the precursor fiber is responsible for the weight loss (Ref 36). Finally, the carbon fiber maintains 87% of original weight compared with 93% of milled carbon microfiber at 1000 °C. It may be explained as the impurity and unstable functional groups, derived from carbon fiber precursor, were probably removed or transformed during the pan-milling.

4. Conclusions

To enhance the efficiency of ready-made milling equipment, carbon microfiber was prepared from short carbon fiber by self-made pan-mill type equipment. SEM observation showed carbon microfiber was produced within a few milling cycles. The particle size reduction and the specific surface area increasing took place simultaneously. The average particle size reduced to 12.7 μm and the specific surface area increased to 0.6 m^2/g after 40 milling cycles. Infrared spectroscopy and XPS indicated that carbon microfiber had more oxygen-containing functional groups than the original sample. XRD illustrated that the crystalline ordered units reduced and crystal type did not change after milling. In addition, microfiber was proved to have a higher thermal stability.

For the manufacture of carbon microfiber, compared with ball-milling, pan-milling approach is more efficient, more convenient and easy to be industrialized, and the resulting product is with improved quality due to its microstructure and mechanochemically functionalized surface.

References

1. M. Endo, C. Kim, K. Nishimura, T. Fujino, and K. Miyashita, Recent Development of Carbon Materials for Li Ion Batteries, *Carbon*, 2000, **38**(2), p 183–197
2. K. Shindo, T. Kondo, and Y. Sakurai, Dependence of Hydrogen Storage Characteristics of Mechanically Milled Carbon Materials on Their Host Structures, *J. Alloys Compd.*, 2004, **372**(1–2), p 201–207
3. E.P. Sheshin, Field Emission of Carbon Fibers, *Ultramicroscopy*, 1999, **79**(1–4), p 101–108
4. H. Sugie, M. Tanemura, V. Filip, K. Iwata, K. Takahashi, and F. Okuyama, Carbon Nanotubes as Electron Source in an X-Ray Tube, *Appl. Phys. Lett.*, 2001, **78**(17), p 2578–2580
5. Y. Saito, K. Hamaguchi, R. Mizushima, S. Uemura, T. Nagasako, J. Yotani, and T. Shimojo, Field Emission from Carbon Nanotubes and Its Application to Cathode Ray Tube Lighting Elements, *Appl. Surf. Sci.*, 1999, **146**(1–4), p 305–311
6. N.S. Xu, Z.S. Wu, S.Z. Deng, and J. Chen, High-Voltage Triode Flat-Panel Display Using Field-Emission Nanotube-Based Thin Films, *J. Vac. Sci. Technol. B*, 2001, **19**(4), p 1370–1372
7. E.C. Botelho, C.L. Nogueira, and M.C. Rezende, Monitoring of Nylon 6,6/Carbon Fiber Composites Processing by X-Ray Diffraction and Thermal Analysis, *J. Appl. Polym. Sci.*, 2002, **86**(12), p 3114–3119
8. T. McNally, P. Boyd, C. McClory, D. Bien, I. Moore, B. Millar, J. Davidson, and T. Carroll, Recycled Carbon Fiber Filled Polyethylene Composites, *J. Appl. Polym. Sci.*, 2008, **107**(3), p 2015–2021
9. N. Chand and A.M. Naik, Development and High Stress Abrasive Wear Behavior of Milled Carbon Fiber-Reinforced Epoxy Gradient Composites, *Polym. Compos.*, 2008, **29**(7), p 736–744
10. T. Sugama and K. Gawlik, Milled Carbon Microfiber-Reinforced Poly(phenylenesulfide) Coatings for Abating Corrosion of Carbon Steel, *Polym. Polym. Compos.*, 2003, **11**(3), p 161–170
11. M.S. Sánchez-Adsuar, A. Linares-Solano, D. Cazorla-Amorós, and L. Ibarra-Rueda, Influence of the Nature and the Content of Carbon Fiber on Properties of Thermoplastic Polyurethane-Carbon Fiber Composites, *J. Appl. Polym. Sci.*, 2003, **90**(10), p 2676–2683
12. S. Carneiro and J.M. Maia, Rheological Behavior of (Short) Carbon Fiber/Thermoplastic Composites. Part I: The Influence of Fiber Type, Processing Conditions and Level of Incorporation, *Polym. Compos.*, 2000, **21**(6), p 960–969
13. J.L. Li, L.J. Wang, and W. Jiang, Carbon Microspheres Produced by High Energy Ball Milling of Graphite Powder, *Appl. Phys. A*, 2006, **83**(3), p 385–388
14. E.P. Sheshin, A.S. Baturin, K.N. Nikolskiy, R.G. Tchesov, and V.B. Sharov, Field Emission Cathodes Based on Milled Carbon Fibers, *Appl. Surf. Sci.*, 2005, **251**(1–4), p 196–200
15. W.G. Shao, Q. Wang, F. Wang, and Y.H. Ch, The Cutting of Multi-Walled Carbon Nanotubes and Their Strong Interfacial Interaction with Polyamide 6 in the Solid State, *Carbon*, 2006, **44**(13), p 2708–2714
16. N.J. Welham, V. Berbenni, and P.G. Chapman, Increase Chemisorption onto Activated Carbon After Ball-Milling, *Carbon*, 2002, **40**(13), p 2307–2315

17. X. Xu and Q. Wang, Mechanochemical Reactor, CN Patent ZL95111258.9, 1995
18. X. Xu, Q. Wang, X.A. Kong, X.D. Zhang, and J.G. Huang, A Pan-Mill Type Equipment Designed for Polymer Stress Reactions: Theoretical Analysis of Structure and Milling Process of the Equipment, *Plast. Rubber Compos. Process. Appl.*, 1996, **25**(3), p 152–158
19. C. Lu and Q. Wang, Preparation of Ultrafine Polypropylene/Iron Composite Powders Through Pan-Milling, *J. Mater. Process. Technol.*, 2004, **145**(3), p 336–344
20. M. Liang, C. Lu, Y. Huang, and C. Zhang, Morphological and Structural Development of Poly(ether ether ketone) During Mechanical Pulverization, *J. Appl. Polym. Sci.*, 2007, **106**(6), p 3895–3902
21. W. Zhang, M. Liang, and C. Lu, Morphological and Structural Development of Hardwood Cellulose During Mechanochemical Pretreatment in Solid State Through Pan-Milling, *Cellulose*, 2007, **14**, p 447–456
22. http://rsb.info.nih.gov/ij/download.html
23. http://www.phy.cuhk.edu.hk/~surface/XPSPEAK/
24. G. Zhang, S. Sun, D. Yang, J.-P. Dodelet, and E. Sacher, The Surface Analytical Characterization of Carbon Fibers Functionalized by H_2SO_4/HNO_3 Treatment, *Carbon*, 2008, **46**(2), p 196–205
25. Y.Z. Wan, Y.L. Wang, F.G. Zhou, G.X. Cheng, and K.Y. Han, Three-Dimensionally Braided Carbon Fiber-Epoxy Composites, a New Type of Materials for Osteosynthesis Devices. II. Influence of Fiber Surface Treatment, *J. Appl. Polym. Sci.*, 2002, **85**(5), p 1040–1046
26. H. Pan, L. Liu, Z.-x. Guo, L. Dai, F. Zhang, D. Zhu, R. Czerw, and D.L. Carroll, Carbon Nanotubols from Mechanochemical Reaction, *Nano Lett.*, 2003, **3**(1), p 29–32
27. X.-X. Zhang, C.-H. Lu, and M. Liang, Preparation of Rubber Composites Form Ground Tire Rubber Reinforced with Waste-Tire Fiber Through Mechanical Milling, *J. Appl. Polym. Sci.*, 2007, **103**(6), p 4087–4094
28. S.-J. Park and B.-J. Kim, Roles of Acidic Functional Groups of Carbon Fiber Surfaces in Enhancing Interfacial Adhesion Behavior, *Mater. Sci. Eng. A*, 2005, **408**(1–2), p 269–273
29. Z.R. Yue, W. Jiang, L. Wang, and S.D. Gardner, Surface Characterization of Electrochemically Oxidized Carbon Fibers, *Carbon*, 1999, **37**(11), p 1785–1796
30. Y.G. Ko, U.S. Choi, J.S. Kim, and Y.S. Park, Novel Synthesis and Characterization of Activated Carbon Fiber and Dye Adsorption Modeling, *Carbon*, 2002, **40**(14), p 2661–2672
31. S,-J. Zhang, H.-M. Feng, J.-P. Wang, and H.-Q. Yu, Structure Evolution and Optimization in the Fabrication of PVA-Based Activated Carbon Fibers, *J. Colloid Interface Sci.*, 2008, **321**(1), p 96–102
32. B. Xu, X. Wang, and Y. Lu, Surface Modification of Polyacrylonitrile-Based Carbon Fiber and Its Interaction with Imide, *Appl. Surf. Sci.*, 2006, **253**(5), p 2695–2701
33. S.D. Gardner, C.S.K. Singamsetty, G.L. Booth, G.-R. He, and C.U. Pittman, Jr., Surface Characterization of Carbon Fibers Using Angle-Resolved XPS and ISS, *Carbon*, 1995, **33**(5), p 587–595
34. U. Zielke, K.J. Hüttinger, and W.P. Hoffman, Surface Oxidized Carbon Fibers: II. Chemical Modification, *Carbon*, 1996, **34**(8), p 999–1005
35. H. Zhou, Q. Yu, Q. Peng, H. Wang, J. Chen, and Y. Kuang, Catalytic Graphitization of Carbon Fibers with Electrodeposited Ni–B Alloy Coating, *Mater. Chem. Phys.*, 2008, **110**(2–3), p 434–439
36. S. Wang, Z.-H. Chen, W.-J. Ma, and Q.-S. Ma, Influence of Heat Treatment on Physical-Chemical Properties of PAN-Based Carbon Fiber, *Ceram. Int.*, 2006, **32**(3), p 291–295